REVISED MANUSCRIPT

A high-precision U–Pb age constraint on the Rhynie Chert Konservat-Lagerstätte: timescale and other implications

S. F. PARRY [1,2], S. R. NOBLE [1], Q. G. CROWLEY [3] & C. H. WELLMAN [4]

[1] *NERC Isotope Geosciences Laboratory, British Geological Survey, Kingsley Dunham Centre, Keyworth, Nottingham NG12 5GG, UK*

[2] *British Geological Survey, Kingsley Dunham Centre, Keyworth, Nottingham NG12 5GG, UK (e-mail: sparry@bgs.ac.uk)*

[3] *School of Natural Sciences, Department of Geology, Trinity College, Dublin 2, Ireland*

[4] *Department of Animal and Plant Sciences, University of Sheffield, Alfred Denny Building, Western Bank, Sheffield S10 2TN, UK*

Corresponding author: SFP

Words of text = *c.* 5480 in total (determined using Word's 'Word Count' tool)
References = 44
Figures = 6 in total (Figs. 1–5 and Fig. SUP 1)
Tables = 2

Supplementary material:
(1) Analytical techniques (ID–TIMS U–Pb geochronology)
(2) Photomicrographs (taken under ethanol) of zircon and titanite grains/grain fragments recovered from the Milton of Noth Andesite

is available at:
(1) http://www.geolsoc.org.uk/SUP18463
(2) http://www.geolsoc.org.uk/SUP18463

Running header: A U–PB AGE CONSTRAINT ON THE RHYNIE CHERT (= 41 characters incl. spaces)
Alternatives: U–PB AGE CONSTRAINT ON THE RHYNIE CHERT (= 39 characters incl. spaces) or RHYNIE CHERT U–PB AGE CONSTRAINT (= 32 characters incl. spaces)

Abstract: An ID-TIMS U–Pb zircon age of 411.5 ± 1.3 Ma obtained from an andesitic lava occurring within the Lower Devonian Rhynie Outlier (Aberdeenshire, NE Scotland) effectively dates the Rhynie Chert Konservat-Lagerstätte. Biostratigraphical constraints on the Rhynie Chert-bearing succession indicate that this age lies within the interval early (but not earliest) Pragian–(?)earliest Emsian. Accordingly, the Pragian–Emsian boundary must post-date or closely approximate to 411.5 ± 1.3 Ma, while the Lochkovian–Pragian boundary must pre-date 411.5 ± 1.3 Ma.

Integration of this new, high-precision age with an improved temporal framework for late Caledonian intrusive activity in NE Scotland suggests that the Rhynie hot-spring system (the 'parental' hydrothermal system to the Rhynie cherts) was unrelated to any 'Newer Granite' intrusion. Rhynie was instead powered by a basaltic andesite magma whose generation and ascent were directly linked to the transcurrent fault movements responsible for the formation of the Rhynie basin. (END OF ABSTRACT)

The Lower Devonian Rhynie Outlier of Aberdeenshire, NE Scotland (Fig. 1) hosts some 50 fossil siliceous sinter horizons which together constitute the Rhynie Chert Konservat-Lagerstätte. These fossil sinter horizons (the 'Rhynie cherts') preserve, in exquisite and unrivalled detail, an almost complete early terrestrial ecosystem (e.g. Trewin 2004; Fayers & Trewin 2004), thus affording a key insight into the emergence of land-based life. Furthermore, the Rhynie cherts represent the surficial expression of a precious metal-bearing hydrothermal system (Rice *et al.* 1995, 2002). Highly anomalous concentrations of Au – along with As, Mo and W – are present within the structurally complex and (in part) pervasively-altered chert-bearing succession. With a biostratigraphical age of early (but not earliest) Pragian to (?)earliest Emsian (Wellman 2004, 2006), Rhynie currently ranks as the oldest known example of a subaerial hot-spring system.

Geochronological constraints on the Rhynie Chert Konservat-Lagerstätte are at present limited to an $^{40}Ar/^{39}Ar$ isochron age of 396 ± 12 Ma (1σ) obtained from the Chert itself (Rice *et al.* 1995) and a more robust weighted mean $^{40}Ar/^{39}Ar$ plateau age of 403.9 ± 2.1 Ma (2σ; relative to Taylor Creek Rhyolite and Fish Canyon Tuff sanidine ages of 27.92 Ma and 28.02 Ma, respectively) deriving from the analysis of vein-hosted hydrothermal K-feldspar and hydrothermally altered andesite (Mark *et al.* 2011). We have therefore undertaken an ID–TIMS U–Pb geochronological study aimed at producing a reliable, accurate and precise radiometric age constraint on the Rhynie Chert-bearing succession, and in so doing permit the assessment of the existing geochronological data and increase confidence in the numerical age assigned to the Rhynie fossil assemblage. This study formed part of a broader re-investigation of the timing of 'late

Caledonian' igneous activity in NE Scotland – a sound knowledge of which is essential to our general understanding of the Rhynie hot-spring system. We herein report on one key aspect of the resultant dataset viz. a high-precision zircon age yielded by an andesitic lava flow occurring within the Rhynie Outlier. We proceed to explore the implications of this age both for the Rhynie Chert and the Devonian timescale, and finally use it to discuss a genetic model for the Rhynie hot-spring system and its concomitant mineralization.

Geological setting

The solid geology of NE Scotland is dominated by Caledonian metamorphic and igneous rocks. These are locally overlain by (?)Siluro-Devonian sediments of Old Red Sandstone (ORS) lithofacies. Caledonian and ORS lithologies alike are cut by several discontinuous E–ENE-trending quartz-dolerite dykes of Permo-Carboniferous age. The ORS sediments are most extensively developed along the Moray Firth coast (representing the southern margin of the Orcadian Basin), but also occur within a number of discrete outliers (Stephenson & Gould 1995; Trewin & Thirlwall 2002) e.g. the Rhynie Outlier (Fig. 1). This particular outlier is an almost entirely fault-bounded, dog-legged (N–S to NE–SW trending) Lower ORS basin of approximately 21 km in length by a maximum of 3 km in width (Gould 1997; Rice & Ashcroft 2004). The basin fill comprises a *c.* 1.5 km thick sequence of fluvio-lacustrine conglomerates, sandstones and shales, with local intercalations of andesitic lavas and tuffs. Surrounding and underlying the Rhynie Outlier are a variety of Ordovician (≥ *c.* 471.5 Ma) igneous rocks (i.e. the 'main' and 'Boganclogh' sectors of the predominantly mafic Insch Pluton, the granitoid Kennethmont Complex, and a suite of granitic minor intrusions; Gould 1997; Parry 2004) and metasediments of the Neoproterozoic to Lower/Middle Cambrian Dalradian Supergroup (British Geological Survey 1993, 2001; Fletcher & Rushton 2008). Also present in the Rhynie area, and common throughout NE Scotland generally, are essentially undeformed granitoid plutonic complexes and (?)associated intermediate-to-acidic minor intrusions (see Stephenson & Gould 1995; Stephenson *et al.* 1999; Parry 2004). Emplaced after the Grampian tectonometamorphic event (i.e. post-*c.* 470 Ma), these bodies typify the 'Newer Granites' of Read (1961).

Though exposure is poor, the stratigraphy and structure of the northern half of the Rhynie Outlier are reasonably well known owing to a comprehensive programme of pitting, trenching and drilling (Rice *et al.* 1995, 2002; Rice & Ashcroft 2004). Three stratigraphic units are recognized (Rice & Ashcroft 2004; see Fig. 2). A 'lower unit' (> 700 m thick) of red–brown sandstones, with local intercalations of red and grey

shales, conglomerates and andesitic lava, is succeeded by a 'middle unit' (> 300 m thick) of grey–green laminated shales, micaceous siltstones and subordinate thin sandstones. This 'middle unit' is in turn overlain by an 'upper unit' (> 300 m thick) of grey–green flaggy sandstones and shales. The 'lower unit' is termed the Tillybrachty Sandstone Formation (and now includes the Quarry Hill Sandstone Formation cf. Gould 1997), while the 'middle' and 'upper' units are each afforded member status – the Windyfield Shales Member and the Milton Flags and Shales Member, respectively – and together comprise the Dryden Flags Formation (cf. Gould 1997). It is believed that the Rhynie cherts occur within the Windyfield Shales Member i.e. within the lower part of the Dryden Flags Formation.

Lavas are best developed in the east and north of the Rhynie Outlier (Fig. 1), where they have a vertical extent of > 100 m. These typically pale brown, porphyritic, vesicular or amygdaloidal rocks (Rice *et al.* 1995; Parry 2004) are thought to occupy a stratigraphic position close to the base of the Tillybrachty Sandstone Formation, although exceptions may exist e.g. the Milton of Noth Andesite (see below). A substantial thickness (> 140 m) of tuffaceous sediment present around Longcroft [NJ 4961 2836] – the so-called Longcroft Tuffs (Rice *et al.* 2002) – is interpreted as the erosional product of intra-Tillybrachty Sandstone Formation lava flows (Rice & Ashcroft 2004), but notably does contain air-fall material (Rice *et al.* 2002).

Biostratigraphy

Plant and arthropod remains preserved within the Rhynie cherts are of little biostratigraphical value. Spores recovered from the associated sedimentary succession are diagnostic of age, however. Horizons occurring within the Tillybrachty Sandstone Formation (including a fine-grained sandstone from within the Longcroft Tuffs), the Windyfield Shales Member, and the Milton Flags and Shales Member have yielded spore assemblages which are similar, and indicate an early (but not earliest) Pragian to (?)earliest Emsian age (*polygonalis-emsiensis* Spore Assemblage Biozone of Richardson & McGregor 1986; Wellman 2004, 2006). This biostratigraphical age range is potentially further constrained by the presence of *Dictyotriletes subgranifer* (Wellman 2006). The occurrence of this particular taxon permits correlation of the Rhynie spore assemblages with the Su Interval Zone of the PoW Oppel Zone (Streel *et al*. 1987), thereby indicating a latest Pragian to (?)earliest Emsian age. For reasons considered by Wellman (2006), it is probably wise, however, to adopt a conservative stance and employ the wider biostratigraphical age range. Nonetheless, it remains the case that the sediments lying below, at, and above the stratigraphic level of the Rhynie cherts fall within the same biostratigraphic interval.

The Milton of Noth Andesite

Field relations

The Milton of Noth Andesite (Rice *et al.* 2002; Parry 2004) is a moderately altered mass of basaltic andesite which extends along the northwestern margin of the Rhynie Outlier between Milton of Noth [NJ 5029 2904] and Newnoth [NJ 5172 3020] (Rice & Ashcroft 2004; Fig. 1). This body has no surface outcrop and is known only from geophysical investigations and pitting/trenching. For the most part, the Andesite exists as a lava flow, although locally e.g. around [NJ 5049 2922], it displays sill-like characteristics (presumably evidencing near-surface burrowing by the advancing flow). Amongst the lavas of the Rhynie Outlier, the Milton of Noth Andesite is unique in that the contact between it and its associated sediments is undoubtedly not erosional in nature. Several features observed in the vicinity of Milton of Noth point to an 'intrusive' lava–sediment contact within an overall conformable context (Parry 2004). Lobe-like protrusions of coherent vesicular lava extend outwards into the surrounding sediment, with one such lobe possessing a sediment wrapping that is in-curled on the Andesite side. At another locality, sandstone bedding is both truncated and exploited by the lava, with sediment pieces locally being isolated by lava. Also frequently developed close to the lava–sediment interface is an incoherent rubble comprising angular fragments and 'balls' of lava mixed with structureless sediment; the incoherent rubble *and* true sediment located within *c.* 0.5 m of the lava are variably vesiculated. On the basis of these field relationships, we conclude that the Milton of Noth Andesite possesses a peperitic marginal facies (e.g. Doyle 2000) indicative of the mixing of magma and 'wet' (i.e. un- or partially lithified) sediment. Eruption of the Milton of Noth Andesite can thus be regarded as having been essentially synchronous with the deposition of its associated sediments (at least at the resolution of U–Pb geochronology).

The sediments themselves that abut the Milton of Noth Andesite are moderately to steeply south- or SE-dipping, grey–green and brownish grey, thinly bedded, fine-grained micaceous sandstones, micaceous siltstones and shales. Sediments such as these occur within both the Tillybrachty Sandstone Formation and the overlying Dryden Flags Formation (particularly the latter), hence it is uncertain to which of the two units the Andesite-associated sediments actually belong. The sediments in question pass southeastwards (i.e. up-succession) over a few tens of metres, and with no detected break, into strata of undoubted Dryden Flags Formation parentage (specifically, the Milton Flags and Shales Member; Rice & Ashcroft 2004). This points strongly to their being part of the Dryden Flags Formation, but it remains the case that all of the other Rhynie Outlier lavas sit within the Tillybrachty Sandstone Formation. One of four stratigraphic positions may therefore be occupied by the Milton of Noth Andesite (Fig. 2): (1) and (2) well within the Dryden Flags Formation (Rice *et al.* 2002), above or below the Rhynie cherts; (3) close to

the boundary between the Dryden Flags and Tillybrachty Sandstone formations (Parry 2004); or (4) near to the base of the Tillybrachty Sandstone Formation (Rice & Ashcroft 2004). This uncertainty over the exact stratigraphic position of the Milton of Noth Andesite fortunately has no detrimental impact on the present study as both the Tillybrachty Sandstone and Dryden Flags formations have consistently yielded spores belonging to the *polygonalis-emsiensis* Spore Assemblage Biozone (see preceding section).

Sample details

A 17 kg sample of the Milton of Noth Andesite was obtained from temporary exposures created on farmland at [NJ 5029 2904] (Fig. 1). This sample, designated RM-15, was taken *c.* 10 m from the lava–sediment contact, in the direction of the interior of the flow (i.e. well clear of the peperitic marginal facies).

Some months later, a second sample of the Milton of Noth Andesite was sought in order to provide an additional supply of suitable dating material. Unfortunately, due to access restrictions, it proved impossible to return to the original sample locality. The nearest alternative locality – 270 m to the NE (i.e. along strike) at [NJ 5049 2922] – was thus identified, and the lava exposed by excavation. On this occasion, a *c.* 150 kg sample (designated RM-15XX; see Fig. 1) was taken 15 m from the lava–sediment interface.

U–Pb geochronology

Conventional ID–TIMS U–Pb geochronology was performed at the NERC Isotope Geosciences Laboratory (NIGL). Full details of the analytical procedure are provided in Supplementary Publication 18463 (available at http://www.geolsoc.org.uk/SUP18463). The resultant data are presented in Table 1 and depicted in Fig. 3. We have attempted to make allowances for all sources of systematic error in our 'final age' calculations, and in accordance with this policy report the age of the Milton of Noth Andesite in the format: Age ± X(Y)[Z] Ma, where X is the internal or analytical uncertainty in the absence of all systematic error (tracer calibration- and decay constant-related); Y includes the tracer calibration error (a conservative 2σ estimate of 0.10 % for the Pb/U ratio in the tracer) and; Z also includes the ^{238}U decay constant error of Jaffey *et al.* (1971).

Sample RM-15 yielded a small quantity of colourless to pale brown zircon. In addition, variably brown titanite fragments (sometimes faceted) were found in the 1.0 A Frantz® split (see Fig. SUP 1, available at

http://www.geolsoc.org.uk/SUP18463). Inherited grains dominate the morphologically heterogeneous zircon population, there being a profusion of rounded, partially resorbed and skeletal examples (Fig. SUP 1). Rare discoveries of colourless, subhedral to near-euhedral prisms and prism fragments with a simple quadratic cross-section were, however, made in one of the least magnetic Frantz® splits (Fig. SUP 1). These inferably primary grains, which were specifically targeted during picking, commonly carry melt and mineral inclusions.

Sample RM-15XX, like sample RM-15, and despite its considerable size, yielded only a small quantity of zircon. Once again, inherited grains dominate the zircon population, but, as before, inferably primary grains (of prismatic morphology) were found in some of the least magnetic Frantz® splits (Fig. SUP 1). Notably absent, however, were titanite fragments. Instead, several incoherent, readily disaggregated rust-coloured masses were discovered in the more magnetic Frantz® splits. These may well represent the remnants of titanite grains and, if so, would suggest that sample RM-15XX is more altered than sample RM-15.

Ten analyses obtained from the Milton of Noth Andesite are herein presented (Table 1). These ten analyses comprise eight fractions of air- and/or chemically-abraded zircon (fractions 1–3 and 6–10) and two multi-grain fractions of air-abraded titanite (fractions 4 and 5). The analyses of fractions 1–6, along with that of fraction 10, plot on or close to concordia at *c.* 410 Ma (Fig. 3a and 3c). In contrast, the analyses of fractions 7, 8 and 9 (all zircon) are significantly discordant (Fig. 3b), together defining a chord with lower and upper concordia-intercept ages of $409.9^{+7.4}_{-7.3}$ Ma and $1601.2^{+8.5}_{-8.5}$ Ma, respectively (MSWD = 1.03; Monte Carlo simulation; decay constant errors included). The close similarity in age between this lower concordia-intercept and the near-concordant cluster of analyses (fractions 1–6 and 10) strongly suggests that both the lower and upper concordia-intercept ages have geological significance. The discordia defined by fractions 7, 8 and 9 presumably represents a two-component mixing line, with end-members of 'primary zircon growth' and '*c.* 1600 Ma inherited zircon'.

Turning to the near-concordant cluster of zircon analyses (Fig. 3a), it can be seen that chemically-abraded single-grain fractions 3 (RM-15) and 10 (RM-15XX) are centred on concordia at *c.* 411.6 Ma. Fractions 2 (RM-15) and 6 (RM-15XX) overlap these analyses, and the concordia curve within error, but are less precise and have ellipse centres which lie on the underside of concordia. A trace of inheritance and/or Pb-loss *may* affect the analyses of both fractions. Minor Pb-loss (± inheritance) most likely *does* affect air-

abraded multi-grain fraction 1 (RM-15), which is normally discordant and has the lowest $^{206}Pb/^{238}U$ age amongst the zircon analyses.

Fractions 4 and 5, with $^{206}Pb/^{238}U$ ages of 411.6 ± 1.6 Ma and 409.3 ± 1.1 Ma, respectively (Table 1; Fig. 3c), are the oldest of five titanite analyses that we undertook during the course of this study. The remaining three analyses (unpubl. data) have significantly younger $^{206}Pb/^{238}U$ ages of *c.* 310 Ma, *c.* 307 Ma and *c.* 179 Ma. In the absence of a plausible geological explanation for each of these ages, we interpret the RM-15 titanite dataset in terms of Pb-loss. It should be noted, however, that the $^{206}Pb/^{238}U$ age of fraction 4 is identical to that of concordant single-grain zircon analyses 3 and 10.

In summary, zircons from both samples RM-15 and RM-15XX, which on morphological grounds were strong candidates for primary magmatic grains, consistently yield an age of *c.* 410 Ma. The four chemically-abraded zircon analyses that overlap one another and the concordia curve (fractions 2, 3, 6 and 10; Table 1) together give a weighted mean $^{206}Pb/^{238}U$ age of 411.5 ± 1.1(1.2)[1.3] Ma (MSWD = 0.12; Fig. 3a), which we interpret as the crystallization/eruption age of the Milton of Noth Andesite. Titanite from sample RM-15 records a maximum age (411.6 ± 1.6 Ma) which is entirely consistent with the zircon data. This titanite could be of either magmatic or hydrothermal origin, but we suspect the former.

Discussion and conclusions

Age of the Rhynie Chert

The U–Pb zircon age yielded by the Milton of Noth Andesite (411.5 ± 1.3 Ma) serves as the first reliable and precise radiometric age constraint on the sedimentary succession of the Rhynie Outlier. But how does this age relate to the Rhynie cherts, and hence the timing of hot-spring activity at Rhynie? Satisfactorily answering this question calls for a careful consideration of the relative stratigraphic positions of, and the temporal separation between, the Rhynie cherts and the dated basaltic andesite lava flow.

Although uncertainty surrounds the exact stratigraphic position of the Milton of Noth Andesite, both it and the Rhynie cherts occupy the same *polygonalis-emsiensis* Spore Assemblage Biozone (early, but not earliest, Pragian to (?)earliest Emsian). This potentially indicates a close similarity in absolute age, but the biostratigraphic interval in question could span several million years (e.g. Tucker *et al.* 1998).

Establishing an accurate figure for the vertical separation between the Milton of Noth Andesite and the Rhynie cherts is, as already discussed, difficult due to the somewhat uncertain stratigraphic affinities of the sediments associated with the Milton of Noth Andesite. This problem is likely compounded by lateral thickness and facies variations, and syn-sedimentary faulting (both parallel and oblique to the basin long axis), within the Rhynie Outlier (see Rice & Ashcroft 2004). Nonetheless, the 'layer-cake' stratigraphic column of Rice & Ashcroft (2004) – based upon a near-complete E–W basinal traverse – suggests that the maximum vertical separation between the Milton of Noth Andesite and the Rhynie cherts is *c.* 700 m (i.e. correlating the Milton of Noth Andesite with the lower part of the Tillybrachty Sandstone Formation; Fig. 2). Converting this stratigraphic thickness to a meaningful time interval is reliant on the choice of an appropriate average depositional rate (see Parry 2004) and on an assumed absence of significant basin-wide unconformities/disconformities. Whilst it is impossible to estimate with any great confidence the rate of sedimentation in the Rhynie Outlier, sedimentological evidence from the borehole cores, and the characteristics of the sedimentary succession in general, indicate essentially uninterrupted, rapid sediment accumulation; deposition is believed to have kept pace with basin subsidence. Lacustrine laminites, of which no discoveries have been made in the Rhynie Outlier to date, accumulate under markedly different (relatively stable) conditions, and at 'slow' rates. Studies of Scottish ORS lacustrine laminite sequences (e.g. Trewin 1986; Trewin & Davidson 1996) suggest depositional rates of *c.* 0.5 mm/yr. At such rates, *c.* 700 m of the Rhynie Outlier succession would have been deposited in *c.* 1.4 million years – very similar to the error on the U–Pb age of the Milton of Noth Andesite. Considering that this period of time is calculated using a conservative sedimentation rate, it can be stated with some confidence that the U–Pb age yielded by the Milton of Noth Andesite does in fact date the Rhynie cherts, and hence hot-spring activity at Rhynie, *within error*.

The case for there being a close temporal association (<< 1 million years) between the Rhynie cherts and the volcanic activity within the Rhynie Outlier is further strengthened if the 'late Caledonian' intrusive history of NE Scotland is examined. New ID–TIMS U–Pb data concerning the Siluro-Devonian 'Newer Granites' of western and central Aberdeenshire (Parry 2004, unpubl. data) show that these bodies are no younger than *c.* 415 Ma (see also below). This is consistent with emplacement depth (Harrison & Hutchinson 1987) and (palaeo-)topographic evidence which indicate that such intrusions must pre-date the Rhynie Outlier. The absence of coeval intrusive igneous activity implies that (a subsurface expression of) the Rhynie Outlier volcanism drove the hot-spring system. This is highly pertinent to the Rhynie cherts–Milton of Noth Andesite age relationship since both numerical calculations (e.g. Cathles *et al.* 1997) and empirical evidence from the Taupo Volcanic Zone, New Zealand (e.g. Hedenquist 1986) suggest that individual near-surface hydrothermal systems remain active (i.e. are sustained) for at most a few tens of

thousands of years. On this basis alone, the U–Pb age yielded by the Milton of Noth Andesite – with its 1.3 million year uncertainty – must effectively date the Rhynie cherts.

Timescale implications

With the determination of a reliable and precise U–Pb age for the biostratigraphically constrained Rhynie Chert-bearing succession, a new 'stratigraphic tie-point' in the Lower Devonian has been established. Spore assemblages recovered from both the Tillybrachty Sandstone and Dryden Flags formations of the Rhynie Outlier indicate that 411.5 ± 1.3 Ma lies within the interval early (but not earliest) Pragian to (?)earliest Emsian (Wellman 2004, 2006). Accordingly, the Pragian–Emsian boundary must post-date or closely approximate to 411.5 ± 1.3 Ma, while the Lochkovian–Pragian boundary must pre-date 411.5 ± 1.3 Ma.

Several (solely or predominantly) U–Pb-based Devonian timescales have emerged in recent years (Tucker *et al.* 1998; Compston 2000; House & Gradstein 2004; Kaufmann 2006; see Table 2). The most widely utilized of these is that of House & Gradstein (2004), who propose Lochkovian–Pragian and Pragian–Emsian boundary ages of 411.2 ± 2.8 Ma and 407.0 ± 2.8 Ma, respectively. It is immediately apparent that our U–Pb age of 411.5 ± 1.3 Ma for the Rhynie Chert-bearing succession cannot easily be reconciled with the House & Gradstein (2004) timescale, even allowing for the uncertainty assigned to their boundary ages. We note, however, that Kaufmann (2006) identifies shortcomings in the House & Gradstein (2004) timescale (which could account for this discrepancy), suggesting instead a timescale based upon a 'segmented calibration' approach. This alternative timescale places the Lochkovian–Pragian and Pragian–Emsian boundaries at 412.3 ± 3.5 Ma and 409.1 ± 3.8 Ma, respectively. Agreement is thus good with an age of 411.5 ± 1.3 Ma for the interval early (but not earliest) Pragian to (?)earliest Emsian, and we would consequently argue that the Lochkovian–Pragian and Pragian–Emsian boundary ages proposed by Kaufmann (2006) are correct within error. Similarly, our U–Pb age is compatible with the Lochkovian–Pragian (413.5 Ma) and Pragian–Emsian (409.5 Ma) boundary ages proposed by Tucker *et al.* (1998), although we acknowledge the drawbacks of the 'time-scale line method' employed by these authors (see Kaufmann 2006).

Existing $^{40}Ar/^{39}Ar$ age constraints

There are two $^{40}Ar/^{39}Ar$ age constraints on the Rhynie Chert Konservat-Lagerstätte. The first of these, an isochron age of 396 ± 12 Ma (1σ) produced from samples of bulk chert (Rice *et al.* 1995), suffers from its considerable analytical uncertainties. The second is a weighted mean plateau age of 403.9 ± 2.1 Ma (2σ)

generated from two samples of vein-hosted hydrothermal K-feldspar and a sample of hydrothermally altered andesite (Mark *et al.* 2011). In order to account for systematic uncertainties associated with the $^{40}Ar/^{39}Ar$ geochronometer, Mark *et al.* (2011) have recalculated their individual sample ages with reference to the Fish Canyon sanidine (FCs) age of 28.201 Ma (Kuiper *et al.* 2008), thereby producing a "U–Pb comparable" mean age of 407.1 ± 2.2 Ma (2σ). This should be temporally equivalent – to within a maximum of a few tens of thousands of years, at the quoted level of uncertainty – with the U–Pb age presented herein (411.5 ± 1.3 Ma, including tracer calibration- and decay constant-related uncertainties), based upon our understanding of the Rhynie hydrothermal episode and the likelihood that the dated andesitic lava evidences the thermal drive for the hot-spring system. The two ages, however, are clearly not in agreement at the 2σ level. We contend that this discrepancy can at least in part be explained by (an underestimation of) systematic $^{40}Ar/^{39}Ar$ uncertainties i.e. those relating to the age of FCs and/or the value of the total ^{40}K decay constant. With regard to the former, the age of FCs is undergoing revision and consensus has yet to be reached. Three different ages have recently been proposed for this widely used standard – 28.201 ± 0.023 (1σ) Ma by Kuiper *et al.* (2008), 28.305 ± 0.036 (1σ) Ma by Renne *et al.* (2010) and 27.93 Ma by Channell *et al.* (2010) – with the variation in these estimates amounting to a non-trivial *c.* 1.3 % (excluding stated uncertainties). Furthermore, the total ^{40}K decay constant is presently known to only ± 2 % at the 2σ level (Min *et al.* 2000; cf. ^{238}U decay constant uncertainty of 0.107 %, 2σ; Jaffey *et al.* 1971). The impact of the FCs- and decay constant-related uncertainties in the case of Rhynie can be illustrated by recalculating the individual sample ages of Mark *et al.* (2011) using the FCs ages of Kuiper *et al.* (2008), Renne *et al.* (2010) and Channell *et al.* (2010), estimating the overall uncertainty by quadratically propagating the 1.3 % uncertainty associated with the age of FCs and the 2.0 % uncertainty associated with the total ^{40}K decay constant. Weighted mean ages produced from the resultant sample ages (following Mark *et al.* 2011) are shown along with their relevant uncertainties in Fig. 4. It is evident that our U–Pb age and the 'normalized' weighted mean $^{40}Ar/^{39}Ar$ age of Mark *et al.* (2011) are broadly similar, but choice of FCs age and full error propagation are critical. We note that this is an active area of research and until such time as the systematic errors associated with the $^{40}Ar/^{39}Ar$ geochronometer have been fully evaluated, our view would be to caution against the general use of the Mark *et al.* (2011) age for Rhynie, and in particular its use for Devonian timescale purposes. In contrast, the reliability of our U–Pb age is underpinned by a coherent zircon and titanite dataset, effective Pb-loss elimination techniques, sound metrological calibrations and a robust estimate of the ^{238}U decay constant (Jaffey *et al.* 1971).

A genetic model for the Rhynie hot-spring system

Pre-requisites for the establishment of a hot-spring system are open structures (i.e. permeable conduits for hydrothermal fluids) and sources of both water and heat. During Pragian–(?)earliest Emsian times, the

then active Rhynie Fault Zone (Fig. 1) was available to channel hydrothermal fluids, while the un- or only partially lithified fluvio-lacustrine sediments of the Rhynie basin would have provided an ample reservoir of meteoric waters (Rice *et al.* 1995, 2002). With regard to the heat source, stable isotope data, corroborated by fluid inclusion studies, indicate a primary magmatic contribution to the Rhynie hydrothermal fluids (Rice *et al.* 1995; Baron *et al.* 2004; Mark *et al.* 2011). A shallow-crustal magma body was presumably present beneath Rhynie during the hydrothermal episode, acting as the thermal drive for the hot-spring system. But was this magma body: (1) andesitic i.e. a subsurface expression of the volcanic activity recorded in the Rhynie Outlier or; (2) felsic, as suggested by the presence of anomalous concentrations of Mo and W in the hydrothermally altered Rhynie Fault Zone rocks?

Intermediate-to-acidic minor intrusions located in close proximity to the Rhynie Outlier were emplaced at either *c.* 472 Ma (i.e. syn-Grampian) or *c.* 427 Ma, while the 'Newer Granite' plutonic complexes of western and central Aberdeenshire were assembled during latest Silurian to earliest Devonian times (*c.* 421–415 Ma) (Parry 2004, unpubl. data). Intrusions of intermediate-to-acidic composition, in particular the 'late Caledonian' 'Newer Granites', cannot have played a direct role in the Rhynie hydrothermal episode at *c.* 411.5 Ma (this study). The only viable magmatic heat source for the Rhynie hot-spring system, therefore, must be one genetically related to the andesitic lavas and tuffs of the Rhynie Outlier.

A model for the Rhynie basin proposed by Rice & Ashcroft (2004) envisages the development of a pull-apart basin above a release bend or step over associated with a roughly N–NE trending (?)dextral strike-slip fault, which is believed to be, or be inherently related to, a major crustal-scale fracture. Transcurrent, possibly reactivated, movement on this structure during Pragian–(?)earliest Emsian times is thought to have promoted upper mantle decompression sufficient to induce partial melting. The resultant melts, likely ascending along the structure ultimately responsible for their generation, rose to shallow crustal levels where they fed surface volcanism.

The location of both the Rhynie cherts and the most intensely altered, silicified and mineralized stretch of the Rhynie Fault Zone (i.e. the hydrothermal feed for the hot-spring system; Rice *et al.* 2002) coincides with the land surface junction of the Rhynie Fault Zone and the northern contact of the Insch Pluton's Boganclogh sector (IPBS; see Fig. 1). This suggests that the northern contact of the IPBS, which is tectonic and gently northward-dipping (Gallagher 1983), has influenced the location of the Rhynie hot-spring system. The junction at depth of two major structures such as a syn-orogenic shear zone and a

trans-crustal strike-slip fault would certainly represent a potential site for magma ponding. We thus propose that during the transtensional episode responsible for the development of the Rhynie basin (Rice & Ashcroft 2004), a dilatational void was created at the junction of the basin-governing strike-slip fault and the syn-Grampian (*c.* 470 Ma) shear zone which forms the northern margin of the IPBS. In this scenario, the dilatational void would have accommodated an unknown, but substantial, volume of (?)upper mantle-derived basaltic andesite magma. Whilst a significant volume of the magma arriving in the upper crust was erupted via the Rhynie Fault Zone and other active faults, an equally significant volume must have remained at depth in the dilatational void, where it would have cooled and solidified on a timescale likely to have been of the order of several tens of thousands of years (e.g. Cathles *et al.* 1997). Hydrothermal activity was probably triggered when sufficient volumes of groundwater (in the form of Lower ORS sediment pore waters) were available to respond to the sub-basinal thermal input, and when a hydrostatic threshold was reached. As it crystallized, the andesitic magma body released fluids, which migrated upwards and entered the hydrothermal system (Rice *et al.* 1995; Baron *et al.* 2004; Mark *et al.* 2011). Fig. 5 is a schematic NW–SE cross-section of the Rhynie basin during the hydrothermal episode.

As–Au–W–Mo mineralization associated with the Rhynie hydrothermal system was probably derived partly from the sub-basinal andesitic magma body and partly from scavenging of suitable lithologies occurring in the local 'basement'. Sillitoe (1997) and John (2001) describe instances of Au mineralization with a demonstrable link to andesitic magmatism, where the metal input was likely controlled by partitioning of Au into a magma-exsolved fluid (Ulrich *et al.* 1999). By analogy, it can be argued that Au was introduced into the Rhynie system by means of a fluid released by the basaltic andesite magma body. This hypothesis is supported by our discovery of trace fine particulate Au in the Milton of Noth Andesite heavy mineral separates. Since the geochemical behaviour of As is very often allied to that of Au, it seems reasonable to conclude that As too was derived largely from the andesitic magma body. This may also be true for Sb and Hg, concentrations of which reach 17 ppm and 0.4 ppm, respectively, in rocks of the Rhynie Fault Zone (Rice *et al.* 1995). It is less likely that W and Mo were sourced from the andesitic magma, however, due to the fact that these two metals generally show affinity with geochemically evolved granitic magmas (e.g. Borodin 2004). Scavenging from the Rhynie Outlier 'basement' is thus the only realistic alternative (see also Rice *et al.* 1995). The rocks available for scavenging were limited to the various Insch Pluton lithologies occurring in the footwall of the Rhynie Fault Zone (quartz–biotite-norite, syenite/monzonite, serpentinite and microdiorite) and the *c.* 472 Ma texturally variable biotite-microgranites which cut the Insch Pluton (Parry 2004). We note with interest then the existence of geochemical evidence to suggest that anomalous concentrations of Mo and W *are* associated with both the

texturally variable biotite-microgranites and the (volumetrically more important) Insch Pluton syenites (British Geological Survey 1991; Gould 1997; Parry 2004). This potential link between Insch Pluton syenites, in particular, and anomalous Mo and W concentrations is key since syenitic rocks occur immediately NW of the Rhynie Fault Zone, and were found at the base of borehole MRD-6 (located at the heart of the hydrothermal system; Rice *et al.* 1995, 2002). Mo- and W-bearing rocks would thus have been readily available for scavenging when the hot-spring system was active.

(Acknowledgements)

S.F.P. gratefully acknowledges receipt of a research studentship made possible through a bequest to the University of Aberdeen by the late A. G. Lyon. The U–Pb geochronology underpinning this study was funded by NERC (Project IP/683/0301). We thank N. Boulton, J. Duncan, A. Sumner and A. Wood for technical assistance, and J. Mackie for granting access to his land. D. Condon provided valuable input during the preparation of the manuscript, while the incisive reviews of F. Corfu and S. Daly resulted in a more focused and improved final version.

References

Baron, M., Hillier, S., Rice, C. M., Czapnik, K. & Parnell, J. 2004. Fluids and hydrothermal alteration assemblages in a Devonian gold-bearing hot-spring system, Rhynie, Scotland. *Transactions of the Royal Society of Edinburgh: Earth Sciences*, **94**, 309-324.

Borodin, L. S. 2004. Model system of petrochemical and metallogenic trends of granitoids as a basis for the prognosis of Sn, Li, Ta, Nb, W, Mo, and Cu deposits. *Geology of Ore Deposits*, **46**, 1-21.

British Geological Survey 1991. *Regional geochemistry of the East Grampians area.* British Geological Survey, Keyworth, Nottingham.

British Geological Survey. 1993. *Alford. Scotland Sheet 76W. Solid Geology. 1:50 000.* British Geological Survey, Keyworth, Nottingham.

British Geological Survey. 2001. *Huntly. Scotland Sheet 86W. Solid Geology. 1:50 000.* British Geological Survey, Keyworth, Nottingham.

Cathles, L. M., Erendi, A. H. J. & Barrie, T. 1997. How long can a hydrothermal system be sustained by a single intrusive event? *Economic Geology*, **92**, 766-771.

Channell, J. E. T., Hodell, D. A., Singer, B. S. & Xuan, C. 2010. Reconciling astrochronological and $^{40}Ar/^{39}Ar$ ages for the Matuyama-Brunhes boundary and late Matuyama Chron. *Geochemistry Geophysics Geosystems*, **11**, doi:10.1029/2010GC003203.

Compston, W. 2000. Interpretation of SHRIMP and isotope dilution zircon ages for the Palaeozoic time-scale: II. Silurian to Devonian. *Mineralogical Magazine*, **64**, 1127-1146.

Doyle, M. G. 2000. Clast shape and textural associations in peperite as a guide to hydromagmatic interactions: Upper Permian basaltic and basaltic andesite examples from Kiama, Australia. *Australian Journal of Earth Sciences*, **47**, 167-177.

Duffield, W. A. & Dalrymple, G. B. 1990. The Taylor Creek Rhyolite of New Mexico: a rapidly emplaced field of lava domes and flows. *Bulletin of Volcanology*, **52**, 475-487.

Fayers, S. R. & Trewin, N. H. 2004. A review of the palaeoenvironments and biota of the Windyfield chert. *Transactions of the Royal Society of Edinburgh: Earth Sciences*, **94**, 325-339.

Fletcher, T. P. & Rushton, A. W. A. 2008. The Cambrian fauna of the Leny Limestone, Perthshire, Scotland. *Transactions of the Royal Society of Edinburgh: Earth Sciences*, **98**, 199-218.

Gallagher, J. W. 1983. *The north-east Grampian Highlands: an investigation based on new geophysical and geological data*. PhD thesis, University of Aberdeen.

Gould, D. 1997. *Geology of the country around Inverurie and Alford*. Memoir of the British Geological Survey, Sheets 76E and 76W (Scotland).

Harrison, T. N. & Hutchinson, J. 1987. The age and origin of the Eastern Grampians Newer Granites. *Scottish Journal of Geology*, **23**, 269-282.

Hedenquist, J. W. 1986. Geothermal systems in the Taupo Volcanic Zone: their characteristics and relation to volcanism and mineralisation. *Royal Society of New Zealand Bulletin*, **23**, 134-168.

House, M. R. & Gradstein, F. M. 2004. The Devonian period. *In*: Gradstein, F. M., Ogg, J. G. & Smith, A. G. (eds.) *A Geologic Time Scale 2004*. Cambridge University Press, Cambridge, 202-221.

Jaffey, A. H., Flynn, K. F., Glendenin, L. E., Bentley, W. C. & Essling, A. M. 1971. Precision measurement of half-lives and specific activities of ^{235}U and ^{238}U. *Physical Review C: Nuclear Physics*, **4**, 1889-1906.

John, D. A. 2001. Miocene and Early Pliocene epithermal gold–silver deposits in the Northern Great Basin, Western United States: characteristics, distribution and relationship to magmatism. *Economic Geology*, **96**, 1827-1853.

Kaufmann, B. 2006. Calibrating the Devonian Time Scale: A synthesis of U–Pb ID–TIMS ages and condont stratigraphy. *Earth-Science Reviews*, **76**, 175-190.

Kuiper, K. F., Deino, A., Hilgen, F. J., Krijgsman, W., Renne, P. R. & Wijbrans, J. R. 2008. Synchronizing Rock Clocks of Earth History. *Science*, **320**, 500-504.

Ludwig, K. R. 1993. *PBDAT: a computer program for processing Pb-U-Th isotope data (version 1.24)*. United States Geological Survey Open-File Report **88-542**.

Mark, D. F., Rice, C. M., Fallick, A. E., Trewin, N. H., Lee, M. R., Boyce, A., & Lee, J. K. W. 2011. $^{40}Ar/^{39}Ar$ dating of hydrothermal activity, biota and gold mineralization in the Rhynie hot-spring system, Aberdeenshire, Scotland. *Geochimica et Cosmochimca Acta*, **75**, 555-569.

Min, K., Mundil, R., Renne, P. R. & Ludwig, K. R. 2000. A test for systematic errors in $^{40}Ar/^{39}Ar$ geochronology through comparison with U/Pb analysis of a 1.1-Ga rhyolite. *Geochimica et Cosmochimca Acta*, **64**, 73-98.

Parry, S. F. 2004. *Age and underlying cause of hot-spring activity at Rhynie, Aberdeenshire, Scotland.* PhD thesis, University of Aberdeen.

Read, H. H. 1961. Aspects of Caledonian magmatism in Britain. *Liverpool and Manchester Geological Journal*, **2**, 653-683.

Renne, P. R., Swisher, C. C., Deino, A. L., Karner, D. B., Owens, T. L. & DePaolo, D. J. 1998. Intercalibration of standards, absolute ages and uncertainties in $^{40}Ar/^{39}Ar$ dating. *Chemical Geology*, **145**, 117-152.

Renne, P. R., Mundil, R., Balco, G., Min, K. & Ludwig, K. R. 2010. Joint determination of ^{40}K decay constants and $^{40}Ar^*/^{40}K$ for the Fish Canyon sanidine standard, and improved accuracy for $^{40}Ar/^{39}Ar$ geochronology. *Geochimica et Cosmochimca Acta*, **74**, 5349-5367.

Rice, C. M. & Ashcroft, W. A. 2004. The geology of the northern half of the Rhynie Basin, Aberdeenshire, Scotland. *Transactions of the Royal Society of Edinburgh: Earth Sciences*, **94**, 299-308.

Rice, C. M., Ashcroft, W. A., Batten, D. J., Boyce, A. J., Caulfield, J. B. D., Fallick, A. E., Hole, M. J., Jones, E., Pearson, M. J., Rogers, G., Saxton, J. M., Stuart, F. M., Trewin, N. H. & Turner, G. 1995. A Devonian auriferous hot spring system, Rhynie, Scotland. *Journal of the Geological Society, London*, **152**, 229-250.

Rice, C. M., Trewin, N. H. & Anderson, L. I. 2002. Geological setting of the Early Devonian Rhynie cherts, Aberdeenshire, Scotland: an early terrestrial hot spring system. *Journal of the Geological Society, London*, **159**, 203-214.

Richardson, J. B. & McGregor, D. C. 1986. Silurian and Devonian spore zones of the Old Red Sandstone continent and adjacent areas. *Geological Survey of Canada Bulletin*, **364**, 1-79.

Sillitoe, R. H. 1997. Characteristics and controls of the largest porphyry copper–gold and epithermal gold deposits in the circum-Pacific region. *Australian Journal of Earth Sciences*, **44**, 373-388.

Stacey, J. S. & Kramers, J. D. 1975. Approximation of terrestrial lead isotope evolution using a two-stage model. *Earth and Planetary Science Letters*, **26**, 207-221.

Stephenson, D. & Gould, D. 1995. *British Regional Geology: The Grampian Highlands* (4th edition). British Geological Survey, HMSO, London, 261 pp.

Stephenson, D., Bevins, R. E., Millward, D., Highton, A. J., Parsons, I., Stone, P. & Wadsworth, W. J. 1999. *Caledonian Igneous Rocks of Great Britain*. Geological Conservation Review Series **17**. Joint Nature Conservation Committee, Peterborough, 648 pp.

Streel, M., Higgs, K., Loboziak, S., Riegel, W. & Steemans, P. 1987. Spore stratigraphy and correlation with faunas and floras in the type marine Devonian of the Ardenne-Rhenish regions. *Review of Palaeobotany and Palynology*, **50**, 211-229.

Trewin, N. H. 1986. Palaeoecology and sedimentology of the Achanarras fish bed of the Middle Old Red Sandstone, Scotland. *Transactions of the Royal Society of Edinburgh: Earth Sciences*, **77**, 21-46.

Trewin, N. H. 2004. History of research on the geology and palaeontology of the Rhynie area, Aberdeenshire, Scotland. *Transactions of the Royal Society of Edinburgh: Earth Sciences*, **94**, 285-297.

Trewin, N. H. & Davidson, R.G. 1996. An Early Devonian lake and its associated biota in the Midland Valley of Scotland. *Transactions of the Royal Society of Edinburgh: Earth Sciences*, **86**, 233-□46.

Trewin, N. H. & Thirlwall, M. F. 2002. Old Red Sandstone. *In*: Trewin, N. H. (ed.) *The Geology of Scotland* (4th Edition). The Geological Society, London, 213-249.

Tucker, R. D., Bradley, D. C., Ver Straeten, C. A., Harris, A. G., Ebert, J. R. & McCutcheon, S. R. 1998. New U–Pb zircon ages and the duration and division of Devonian time. *Earth and Planetary Science Letters*, **158**, 175-186.

Ulrich, T., Günther, D. & Heinrich, C. A. 1999. Gold concentrations of magmatic brines and the metal budget of porphyry copper deposits. *Nature*, **399**, 676-679.

Wellman, C. H. 2004. Palaeoecology and palaeophytogeography of the Rhynie chert plants: evidence from integrated analysis of *in situ* and dispersed spores. *Proceedings of the Royal Society of London (Series B: Biological Sciences)*, **271**, 985-992.

Wellman, C. H. 2006. Spore assemblages from the Lower Devonian 'Lower Old Red Sandstone' deposits of the Rhynie outlier, Scotland. *Transactions of the Royal Society of Edinburgh: Earth Sciences*, **97**, 167-211.

(END OF REFERENCE LIST)

Figure captions:

Fig. 1. Simplified solid geology of the Rhynie Outlier and surrounding area (based on British Geological Survey 1993 with modifications from Rice & Ashcroft 2004). The inset shows the location of the Rhynie Outlier within NE Scotland. Numbers adjacent to tick marks refer to British National Grid square NJ.

Fig. 2. Generalized stratigraphic column for the northern half of the Rhynie Outlier (after Rice & Ashcroft 2004). The equivalent British Geological Survey (1993) stratigraphic succession is shown for comparison. * Possible stratigraphic positions of the Milton of Noth Andesite (see text for further details).

Fig. 3. U–Pb concordia plots for the Milton of Noth Andesite. **(a)** Concordant and near-concordant zircon analyses (samples RM-15 and RM-15XX). **(b)** Significantly discordant zircon analyses (sample RM-15XX). **(c)** Titanite analyses (sample RM-15). Numerical fraction identifiers correspond to fraction numbers in Table 1. The concordia curve shows ages in Ma, and ellipses indicate 2σ errors.

Fig. 4. Comparison of U–Pb and $^{40}Ar/^{39}Ar$ age constraints on the Rhynie Chert Konservat-Lagerstätte. **(a)** ID–TIMS U–Pb zircon age (this study), including tracer calibration- and decay constant-related uncertainties. **(b)** Weighted mean $^{40}Ar/^{39}Ar$ plateau age of Mark *et al.* (2011) as originally presented (monitor standards used were Taylor Creek Rhyolite sandine and FCs, their ages being taken as 27.92 ± 0.084 Ma and 28.02 ± 0.56 Ma, respectively; Duffield & Dalrymple 1990; Renne *et al.* 1998). **(c)-(e)** Weighted means of the individual sample $^{40}Ar/^{39}Ar$ ages of Mark *et al.* (2011) recalculated with respect to the FCs ages of Kuiper *et al.* (2008), Renne *et al.* (2010) and Channell *et al.* (2010), respectively, and including uncertainty (1.3 %) associated with the age of FCs. **(f)-(h)** As (c)-(e), but also including uncertainty (2 %) associated with the total ^{40}K decay constant (Min *et al.* 2000).

Fig. 5. Schematic NW–SE cross-section of the Rhynie basin (northwestern margin, near Rhynie) at the time of hot-spring activity (modified from Baron *et al.* 2004). The system-powering magma body occupies a dilatational void created at the intersection of the basin-governing strike-slip fault and the shear zone forming the northern margin of the Insch Pluton's Boganclogh sector.

Table captions:

Table 1. U–Pb analytical data.

Table 2. Summary of recently proposed Lochkovian–Pragian and Pragian–Emsian boundary ages.

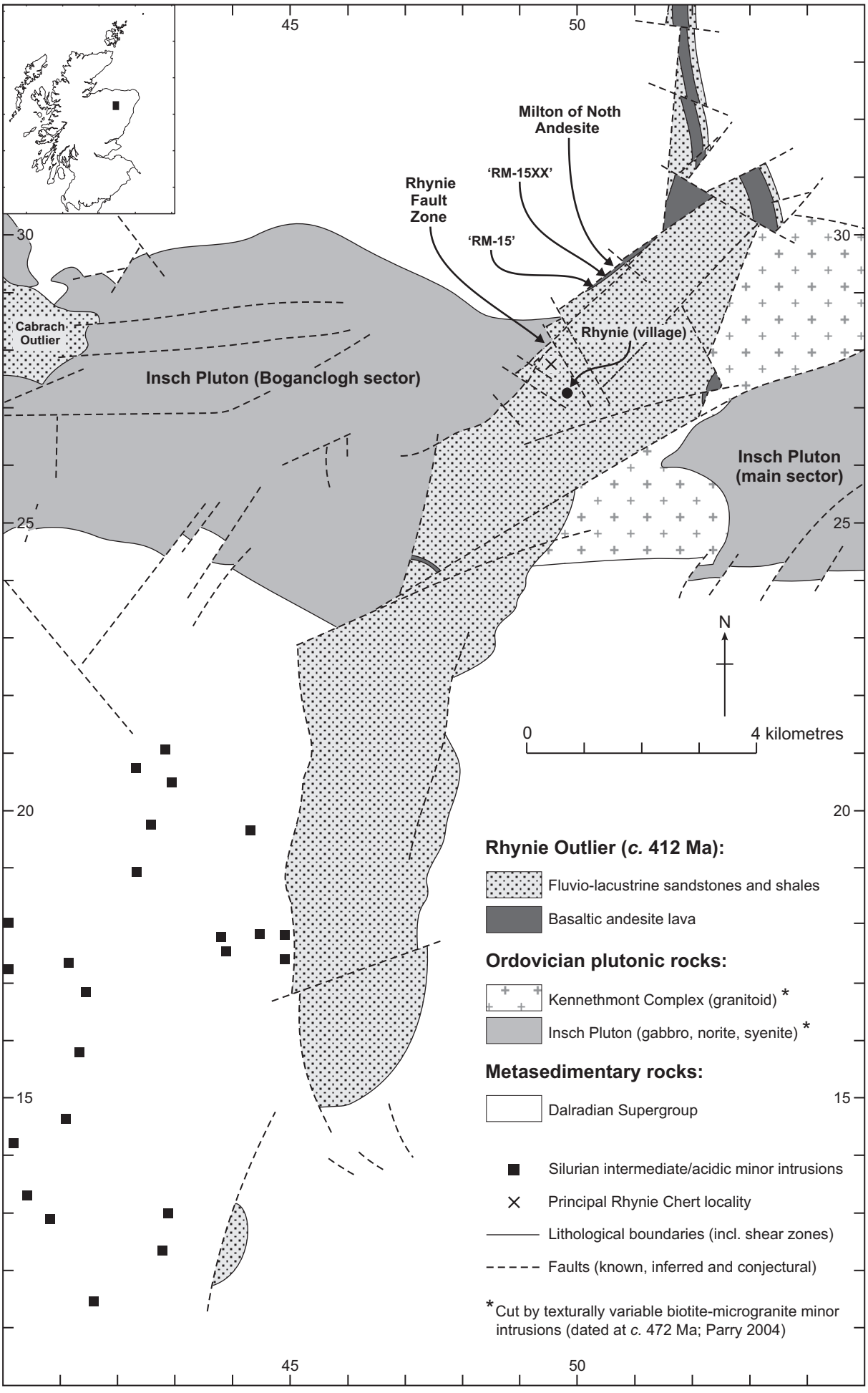
45
50
30
25
20
15
Milton of Noth Andesite
'RM-15XX'
Rhynie Fault Zone
'RM-15'
Rhynie (village)
Cabrach Outlier
Insch Pluton (Boganclogh sector)
Insch Pluton (main sector)
N
0
4 kilometres
Rhynie Outlier (c. 412 Ma):
Fluvio-lacustrine sandstones and shales
Basaltic andesite lava
Ordovician plutonic rocks:
Kennethmont Complex (granitoid) *
Insch Pluton (gabbro, norite, syenite) *
Metasedimentary rocks:
Dalradian Supergroup
Silurian intermediate/acidic minor intrusions
Principal Rhynie Chert locality
Lithological boundaries (incl. shear zones)
Faults (known, inferred and conjectural)
* Cut by texturally variable biotite-microgranite minor intrusions (dated at c. 472 Ma; Parry 2004)

Rhynie Outlier (northern half) stratigraphic succession

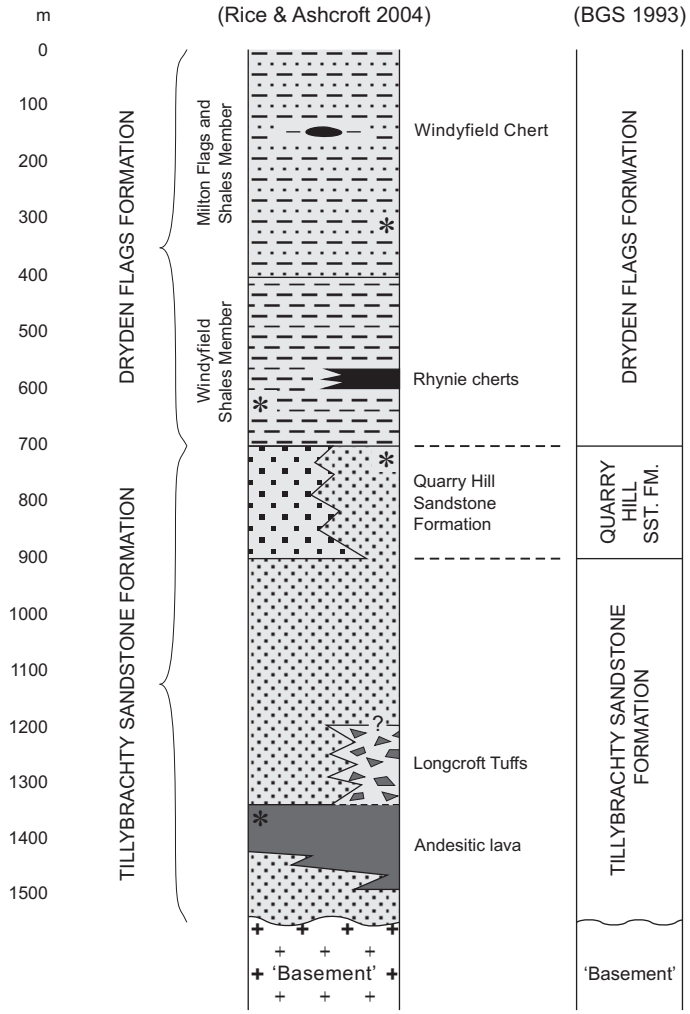

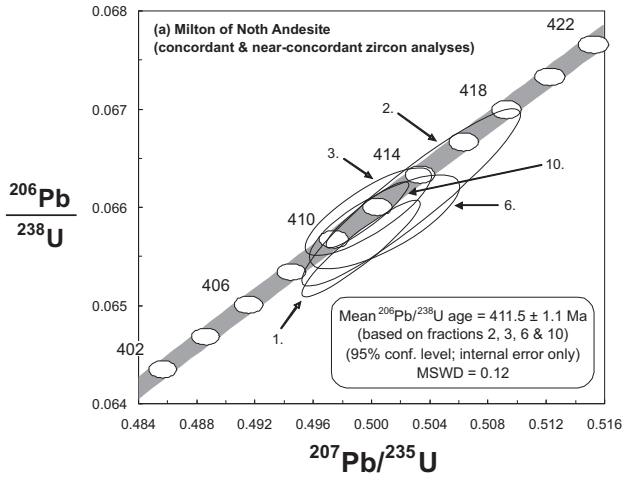
(a) Milton of Noth Andesite
(concordant & near-concordant zircon analyses)
422
418
414
410
406
402
1.
2.
3.
6.
10.
Mean 206Pb/238U age = 411.5 ± 1.1 Ma
(based on fractions 2, 3, 6 & 10)
(95% conf. level; internal error only)
MSWD = 0.12
0.068
0.067
0.066
0.065
0.064
0.484
0.488
0.492
0.496
0.500
0.504
0.508
0.512
0.516
206Pb/238U
207Pb/235U

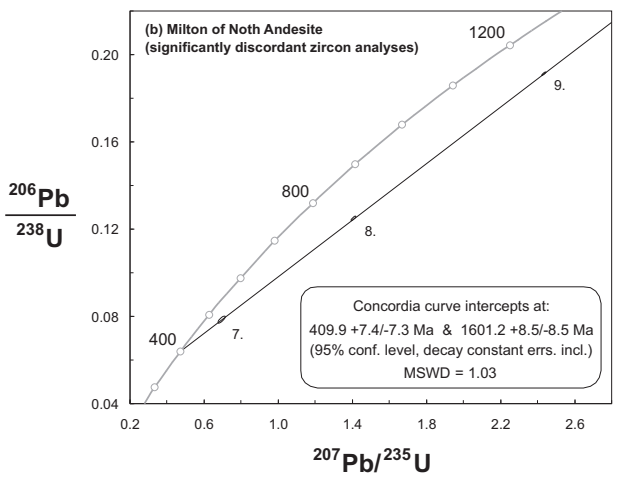
(b) Milton of Noth Andesite
(significantly discordant zircon analyses)
1200
800
400
7.
8.
9.
Concordia curve intercepts at:
409.9 +7.4/-7.3 Ma & 1601.2 +8.5/-8.5 Ma
(95% conf. level, decay constant errs. incl.)
MSWD = 1.03
0.20
0.16
0.12
0.08
0.04
0.2
0.6
1.0
1.4
1.8
2.2
2.6
206Pb/238U
207Pb/235U

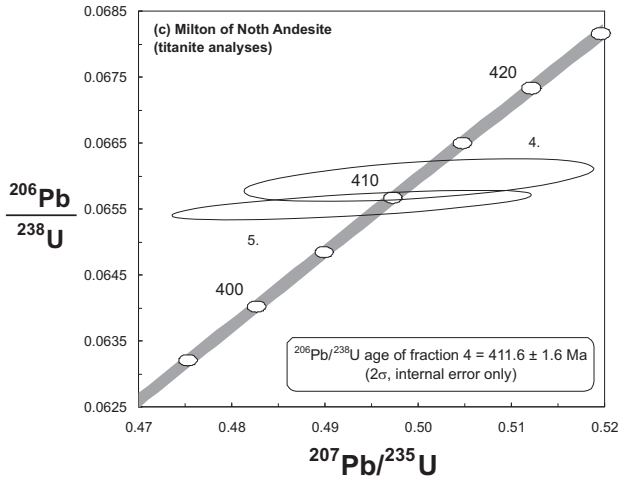
(c) Milton of Noth Andesite
(titanite analyses)
420
410
400
4.
5.
206Pb/238U age of fraction 4 = 411.6 ± 1.6 Ma
(2σ, internal error only)
0.0685
0.0675
0.0665
0.0655
0.0645
0.0635
0.0625
0.47
0.48
0.49
0.50
0.51
0.52
206Pb/238U
207Pb/235U

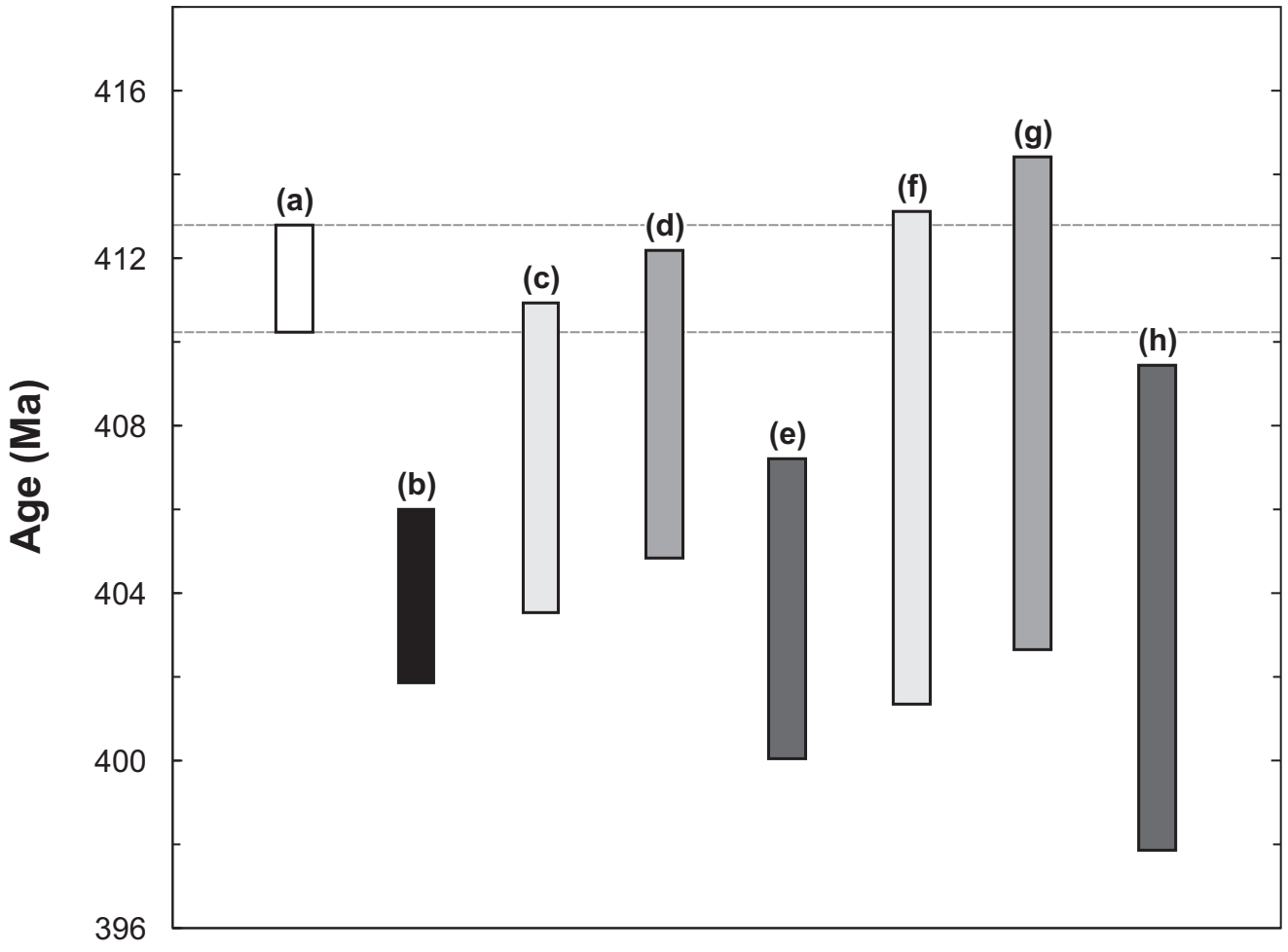
Age (Ma)
416
412
408
404
400
396
(a)
(b)
(c)
(d)
(e)
(f)
(g)
(h)

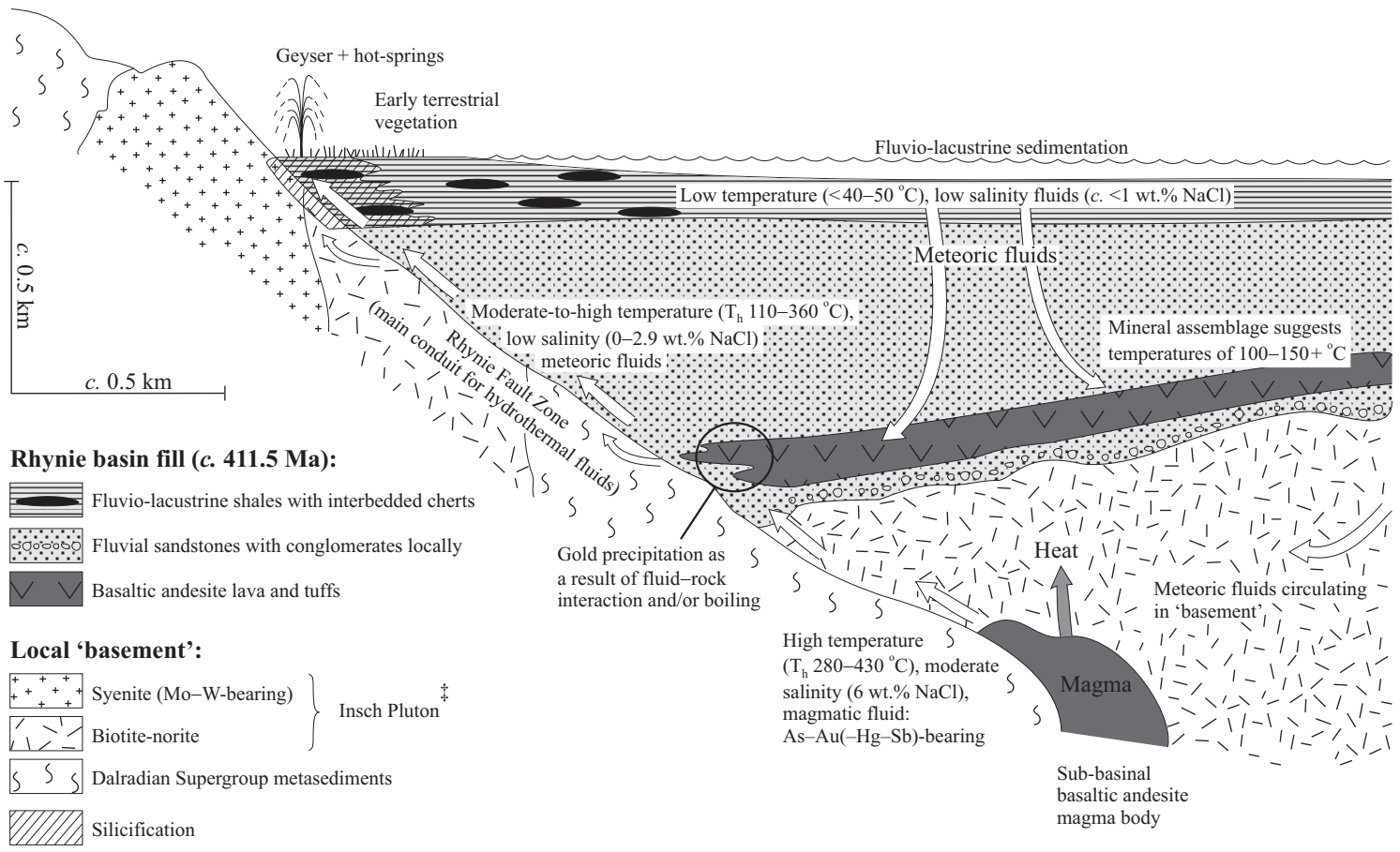

‡ Cut by small bodies of As–W-bearing biotite-microgranite (dated at *c.* 472 Ma; Parry 2004).

Table 1. *U–Pb analytical data*

Fraction number and description*	Weight (mg)	Concentrations† U (ppm)	Concentrations† Pb rad. (ppm)	Measured Tot. cm. Pb (pg)	Measured $^{206}Pb/^{204}Pb$‡	Atomic ratios§ $^{208}Pb/^{206}Pb$	Atomic ratios§ $^{206}Pb/^{238}U$	Atomic ratios§ $^{207}Pb/^{235}U$	Atomic ratios§ $^{207}Pb/^{206}Pb$	Ages (Ma) $^{206}Pb/^{238}U$	Ages (Ma) $^{207}Pb/^{235}U$	Ages (Ma) $^{207}Pb/^{206}Pb$	ρ¶
RM-15 Milton of Noth Andesite sample 1 [NJ 5029 2904]													
1. Z^{aa}, 1.8 A/10°, sm, stb, cl, mti (6)	0.0075	234.3	17.91	8.1	906	0.2982	0.06558 ± 0.62	0.4993 ± 0.67	0.05522 ± 0.25	409.5 ± 2.4	411.2 ± 2.3	421.2 ± 5.6	0.93
2. Z^{ca}, 1.8 A/10°, lrg, el, cl, mli (1)	0.0007[e]	212.6	16.39	1.3	507	0.2991	0.06609 ± 1.12	0.5028 ± 1.22	0.05517 ± 0.44	412.6 ± 4.5	413.6 ± 4.1	419.1 ± 9.8	0.93
3. Z^{ca}, 1.8 A/10°, lrg, stb, cl, mli (1)	0.0071[e]	46.12	3.732	1.9	721	0.3695	0.06595 ± 0.56	0.4998 ± 0.71	0.05497 ± 0.42	411.7 ± 2.2	411.6 ± 2.4	410.8 ± 9.3	0.81
4. T^{aa}, 1.0 A/20°, med–lrg, fr, plbr, mli (15)	0.1213	96.57	15.75	270	195	1.805	0.06593 ± 0.41	0.5002 ± 3.06	0.05503 ± 2.87	411.6 ± 1.6	411.9 ± 10	413.3 ± 64	0.52
5. T^{aa}, 1.0 A/20°, sm–lrg, fr, y–br, mli (26)	0.1004	85.32	12.08	200	195	1.445	0.06555 ± 0.28	0.4930 ± 3.20	0.05455 ± 3.01	409.3 ± 1.1	407.0 ± 11	393.8 ± 68	0.68
RM-15XX Milton of Noth Andesite sample 2 [NJ 5049 2922]													
6. Z^{aa+ca}, nm/10°, lrg, fr, cl, mti (2)	0.0181[e]	109.0	8.707	16	518	0.3530	0.06585 ± 0.60	0.5009 ± 0.84	0.05517 ± 0.56	411.1 ± 2.4	412.3 ± 2.8	419.3 ± 12	0.75
7. Z^{ca}, nm/10°, med–lrg, stb–el, cl (2)	0.0022[e]	225.0	17.99	15	176	0.1222	0.07834 ± 1.85	0.6990 ± 2.37	0.06472 ± 1.39	486.2 ± 8.7	538.2 ± 9.9	765.2 ± 29	0.81
8. Z^{ca}, nm/10°, med, stb–el, ft (2)	0.0016[e]	269.3	32.90	5.5	619	0.05777	0.1247 ± 0.76	1.408 ± 0.79	0.08192 ± 0.20	757.5 ± 5.4	892.5 ± 4.7	1243.7 ± 4.0	0.97
9. Z^{ca}, nm/10°, med, fr, ft, mli (1)	0.0045[e]	154.2	30.92	5.1	1627	0.1270	0.1912 ± 0.34	2.438 ± 0.36	0.09247 ± 0.11	1127.8 ± 3.6	1253.8 ± 2.6	1477.1 ± 2.1	0.95
10. Z^{ca}, 1.8 A/10°, lrg, el, cl, mli (1)	0.0019[e]	247.8	16.99	1.3	1440	0.1539	0.06592 ± 0.42	0.4998 ± 0.46	0.05499 ± 0.19	411.5 ± 1.7	411.6 ± 1.6	411.7 ± 4.2	0.91

* Properties: Z, zircon; T, Titanite; [aa] air-abraded; [ca] chemically-abraded; A, magnet current in amps at specified number of degrees side tilt on a Frantz® LB-1 Magnetic Barrier Separator; nm, non-magnetic at 1.8 amps/specified side tilt on a Frantz® LB-1; sm, small (longest dimension < 80 μm); med, medium-sized (longest dimension 80–150 μm); lrg, large (longest dimension > 150 μm); stb, stubby (applies to prisms with aspect ratios of ≤ 3:1); el, elongate (applies to prisms with aspect ratios upwards of 3:1); fr, fragment(s); cl, colourless; y, yellow; plbr, pale brown; br, brown; ft, faintly coloured (yellowish or rustic); mti, melt inclusions present; mli, mineral inclusions present. Values in parentheses refer to the number of grains analysed.

† Uncertainty in sample weights, and hence U and Pb concentrations, is 20–40 %. Weights were measured on a Cahn® C32 microbalance. [e] denotes weights estimated using a digital imaging system.

‡ Corrected for fractionation (0.10–0.13 % per a.m.u.) and common Pb in the spike only.

§ Corrected for fractionation (0.10 % per a.m.u. in the case of U), spike, laboratory blank Pb and U, and initial common Pb (Stacey & Kramers (1975) model Pb equivalent to the interpreted age of the fraction). Quoted errors are 2σ % for atomic ratios and 2σ absolute for ages. Errors on measured ratios propagated through the data reduction calculations were ± 2 standard errors of the mean. The laboratory blank is believed to have the following isotopic composition: $^{206}Pb/^{204}Pb$:$^{207}Pb/^{204}Pb$:$^{208}Pb/^{204}Pb$ = 17.69:15.58:37.46 (further details are available upon request).

¶ $^{207}Pb/^{235}U$–$^{206}Pb/^{238}U$ error correlation coefficient (Ludwig 1993).

Table 2. *Summary of recently proposed Lochkovian –Pragian and Pragian–Emsian boundary ages*

Devonian timescale reference	Stage boundary age (Ma)				Stage duration (10^6 y)
	Lochkovian–Pragian		Pragian–Emsian		Pragian
Tucker *et al.* (1998)	413.5		409.5		4.0
Compston (2000)	409.4		408.5		0.9
House & Gradstein (2004)	411.2	± 2.8	407.0	± 2.8	4.2
Kaufmann (2006)	412.3	± 3.5	409.1	± 3.8	3.2

Supplementary Publication 18463 (Part 1)

Parent paper:
Parry, S. F., Noble, S. R., Crowley, Q. G. & Wellman, C. H. 2011. A high-precision U–Pb age constraint on the Rhynie Chert Konservat-Lagerstätte: timescale and other implications. *Journal of the Geological Society, London*, **168**, 863–872.

Analytical techniques

ID–TIMS U–Pb geochronology

Conventional ID–TIMS U–Pb geochronology was performed at the NERC Isotope Geosciences Laboratory (NIGL). Bulk samples of the Milton of Noth Andesite (RM-15 and RM-15XX) were first collected as described in the parent paper. These samples were thoroughly washed with water, allowed to dry naturally, then processed using standard crushing and mineral separation techniques. The resultant heavy mineral concentrates were split according to magnetic susceptibility using a Frantz® LB-1 Barrier Separator. Zircon and titanite were subsequently handpicked under ethanol, with only the highest quality, inferably magmatic grains and grain fragments being selected for analysis. Air abrasion (Krogh 1982) and chemical abrasion (Mattinson 2005 with modifications*) were variously employed in an attempt to eliminate the effects of Pb-loss. The individual zircon and titanite fractions were sequentially washed then, having been either weighed or imaged, transferred to Teflon® dissolution vessels (Parrish-type micro-capsules (Parrish 1987) with the exception of fractions 2, 3 and 10, for which miniature Krogh-type bombs (Krogh 1973; Corfu & Noble 1992) were used) ahead of spiking and acidification. Two different isotopic tracer solutions were used during the course of this study: a ^{205}Pb–^{235}U solution (Krogh & Davis 1975) and a ^{205}Pb–^{233}U–^{235}U solution (Parrish & Krogh 1987; see also Monaghan & Parrish 2006). The dissolved, spike-equilibrated fractions were, in general, subjected to ion-exchange procedures. Separation and purification of U and Pb were thus achieved on miniature ion-exchange columns (Corfu & Noble 1992) filled with Bio-Rad AG® 1-X8 (zircon U and Pb, titanite Pb) or Eichrom UTEVA® resin (titanite U), otherwise following the methods of Krogh (1973) with minor modifications (Corfu & Ayres 1984; Corfu & Andrews 1987; Parrish *et al*. 1992). In contrast, chemically-abraded single-grain zircon fractions 2, 3 and 10 underwent a two-stage chloride conversion step (carried out on a hotplate), after which they received no further chemical treatment. U and Pb (± matrix elements) were loaded either separately or together along with silica gel and H_3PO_4 onto single outgassed rhenium filaments and analysed using a Thermo Scientific Triton mass spectrometer (fitted with an axial MasCom secondary electron multiplier) or a VG 354 mass spectrometer (equipped with an axial Daly system comprising a Philips photomultiplier

tube, an Ortec fast pre-amplifier, amplifier-discriminator and pulse counter, and a WARP™ filter). The mass spectrometer output was scrutinized for statistical outliers and evidence of organic interferences using an in-house data evaluation program (Triton output), or done simply by eye (VG 354 output), and any offending data rejected. Thereafter, the measured isotope ratios were corrected for total procedural Pb and U blanks[†] of 1.2–20 pg and 0.50–3.9 pg, respectively, with the Pb composition deriving either from direct laboratory measurements or from the particulate dataset of Noble *et al.* (2008). Pb isotope ratios were further corrected for initial common Pb using a Stacey & Kramers (1975) model Pb composition equivalent to the interpreted age of the individual fractions (a 2 % uncertainty was assigned to these values). All data reduction and plotting were carried out using PBDAT version 1.24 (Ludwig 1993) and Isoplot version 3.00 (Ludwig 2003). The decay constants used were those proposed by Jaffey *et al*. (1971) (Steiger & Jäger 1977). Errors quoted for isotope ratios and ages are at either the 2σ or the 95 % confidence level (Ludwig 1980). Fully corrected analytical data are presented in Table 1 and depicted in Fig. 3 (see parent paper). We have attempted to make allowances for all sources of systematic error in our 'final age' calculations, and in accordance with this policy report the age of the Milton of Noth Andesite in the format: Age ± X(Y)[Z] Ma, where X is the internal or analytical uncertainty in the absence of all systematic error (tracer calibration- and decay constant-related); Y includes the tracer calibration error (a conservative 2σ estimate of 0.10 % for the tracer's Pb/U ratio) and; Z also includes the ^{238}U decay constant error of Jaffey *et al.* (1971).

[*] The selected grains and grain fragments were annealed in small numbers (as opposed to in bulk) in quartz glass beakers at either 850 °C (fractions 6, 7, 8 and 9) or 900 °C (fractions 2, 3 and 10) for *c.* 60 hours. Leaching was subsequently carried out overnight (12–14 hours) at either 160 °C in Teflon® micro-centrifuge tubes (fractions 6, 7, 8 and 9) or 180 °C in 3 ml Savillex vials (fractions 2, 3 and 10) using 29 M HF + trace 8 M HNO_3. The grains/fragments were decanted into pre-cleaned PMP beakers, rinsed several times with Milli-Q® H_2O, then allowed to warm on a hotplate (*c.* 90 °C) in the presence of 3 M HCl for 3–4 hours. After further rinsing with Milli-Q® H_2O and also 8 M HNO_3, the grains/fragments were ready for full dissolution.

[†] For further details see Table SUP 1 below. The observed variation reflects fluctuations in the laboratory blank during the period over which these analyses were performed.

Table SUP 1. *Pb and U blanks for individual fractions*

Fraction number	Pb blank (pg)	U blank (pg)
1.	7.0	0.60
2.	1.2	0.50
3.	1.2	0.50
4.	20	0.75
5.	1.7	3.9
6.	8.0	0.60
7.	8.0	0.60
8.	4.0	0.60
9.	4.0	0.60
10.	1.2	0.50

References

Corfu, F. & Andrews, A. J. 1987. Geochronological constraints on the timing of magmatism, deformation, and gold mineralization in the Red Lake greenstone belt, northwestern Ontario. *Canadian Journal of Earth Sciences*, **24**, 1302–1320.

Corfu, F. & Ayres, L. D. 1984. U–Pb age and genetic significance of heterogeneous zircon populations in rocks from the Favourable Lake area, northwestern Ontario. *Contributions to Mineralogy and Petrology*, **88**, 86–101.

Corfu, F. & Noble, S. R. 1992. Genesis of the southern Abitibi greenstone belt, Superior Province, Canada: evidence from zircon Hf isotope analyses using a single filament technique. *Geochimica et Cosmochimica Acta*, **56**, 2081–2097.

Jaffey, A. H., Flynn, K. F., Glendenin, L. E., Bentley, W. C. & Essling, A. M. 1971. Precision measurement of half-lives and specific activities of ^{235}U and ^{238}U. *Physical Review C: Nuclear Physics*, **4**, 1889–1906.

Krogh, T. E. 1973. A low contamination method for the hydrothermal decomposition of zircon and extraction of U and Pb for isotopic age determinations. *Geochimica et Cosmochimica Acta*, **37**, 485–494.

Krogh, T. E. 1982. Improved accuracy of U–Pb zircon ages by the creation of more concordant systems using an air abrasion technique. *Geochimica et Cosmochimica Acta*, **46**, 637–649.

Krogh, T. E. & Davis, G. L. 1975. The production and preparation of ^{205}Pb for use as a tracer for isotope dilution analysis. *Carnegie Institution of Washington Yearbook* **74**, 416–417.

Ludwig, K. R. 1980. Calculation of uncertainties of U–Pb isotope data. *Earth and Planetary Science Letters*, **46**, 212–220.

Ludwig, K. R. 1993. *PBDAT: a computer program for processing Pb-U-Th isotope data (version 1.24)*. United States Geological Survey Open-File Report **88-542**.

Ludwig, K. R. 2003. *Isoplot 3.00: a geochronological toolkit for Microsoft Excel*. Berkeley Geochronology Center Special Publication **4**.

Mattinson, J. M. 2005. Zircon U–Pb chemical abrasion ("CA-TIMS") method: Combined annealing and multi-step partial dissolution analysis for improved precision and accuracy of zircon ages. *Chemical Geology*, **220**, 47–66.

Monaghan, A. A. & Parrish, R. R. 2006. Geochronology of Carboniferous–Permian magmatism in the Midland Valley of Scotland: implications for regional tectonomagmatic evolution and the numerical time scale. *Journal of the Geological Society, London*, **163**, 15–28.

Noble, S. R., Horstwood, M. S. A., Davy, P., Pashley, V., Spiro, B. & Smith, S. 2008. Evolving Pb isotope signatures of London airborne particulate matter (PM_{10}) – constraints from on-filter and solution-mode MC-ICP-MS. *Journal of Environmental Monitoring*, **10**, 830–836.

Parrish, R. R. 1987. An improved micro-capsule for zircon dissolution in U–Pb geochronology. *Chemical Geology (Isotope Geoscience section)*, **66**, 99–102.

Parrish, R. R. & Krogh, T. E. 1987. Synthesis and purification of ^{205}Pb for U–Pb geochronology. *Chemical Geology (Isotope Geoscience section)*, **66**, 103–110.

Parrish, R. R., Bellerive, D. & Sullivan, R. W. 1992. U–Pb chemical procedures for titanite and allanite in the geochronology laboratory, Geological Survey of Canada. *In*: *Radiogenic Age and Isotope Studies: Report 5*. Geological Survey of Canada Paper **91-02**, 187–190.

Stacey, J. S. & Kramers, J. D. 1975. Approximation of terrestrial lead isotope evolution using a two-stage model. *Earth and Planetary Science Letters*, **26**, 207–221.

Steiger, R. H. & Jäger, E. 1977. Subcommission on geochronology: convention on the use of decay constants in geo- and cosmo-chronology. *Earth and Planetary Science Letters*, **36**, 359–362.

Supplementary Publication 18463 (Part 2)

Parent paper:
Parry, S. F., Noble, S. R., Crowley, Q. G. & Wellman, C. H. 2011. A high-precision U–Pb age constraint on the Rhynie Chert Konservat-Lagerstätte: timescale and other implications. *Journal of the Geological Society, London*, **168**, 863–872.

Figure caption:

Fig. SUP 1. Photomicrographs (taken under ethanol) of zircon and titanite grains/grain fragments recovered from the Milton of Noth Andesite.
(a) Rounded, variably corroded zircons of mixed morphology. Large mineral inclusions and 'rust'-filled cracks are commonplace. Grains such as these are believed to be xenocrysts. (Sample RM-15)
(b) Morphologically variable pieces of essentially colourless zircon. Some mineral inclusions and cracks are observed. These grains/grain fragments are regarded as xenocrysts or suspect xenocrysts. (Sample RM-15)
(c) Further examples of xenocrystic zircon grains/fragments. Extensive cracks and mineral inclusions are observed in some of these. The rounded rim of a large inherited core is discernible in the well-faceted grain located towards the top of the field of view. (Sample RM-15)
(d) Fragments of morphologically simple, colourless, near-euhedral zircon prisms. Axial melt 'tubes' are conspicuous in three of these. Grains/fragments of this type are believed to represent primary zircon growth. The imaged fragments were not analysed, however, owing to the fact that they were reduced to a 'gravel' by the chemical abrasion process. (Sample RM-15)
(e) Fragments of colourless prismatic zircon. A melt inclusion is readily discernible in the lowermost of these. The four pictured fragments were analysed together as Fraction 1. (Sample RM-15).
(f) Colourless/slightly rust-coloured, morphologically simple zircon prisms/prism fragments. Four of these are regarded as xenocrysts or suspect xenocrysts, but the three euhedral/near-euhedral prisms located close to the centre of the field of view are examples of the grains which yield *c.* 411.5 Ma ages. (RM-15XX)
(g) Large, yellowish, yellowish brown or pale brown titanite fragments, one of which is notably well faceted. (Sample RM-15)
(h) Partially faceted, pale brown titanite fragments. Orangey red (?)rutile inclusions are discernible in two of these. (Sample RM-15)

Parry *et al.* **Fig. SUP 1.**